Supplementary Materials

Supplementary Figure 1

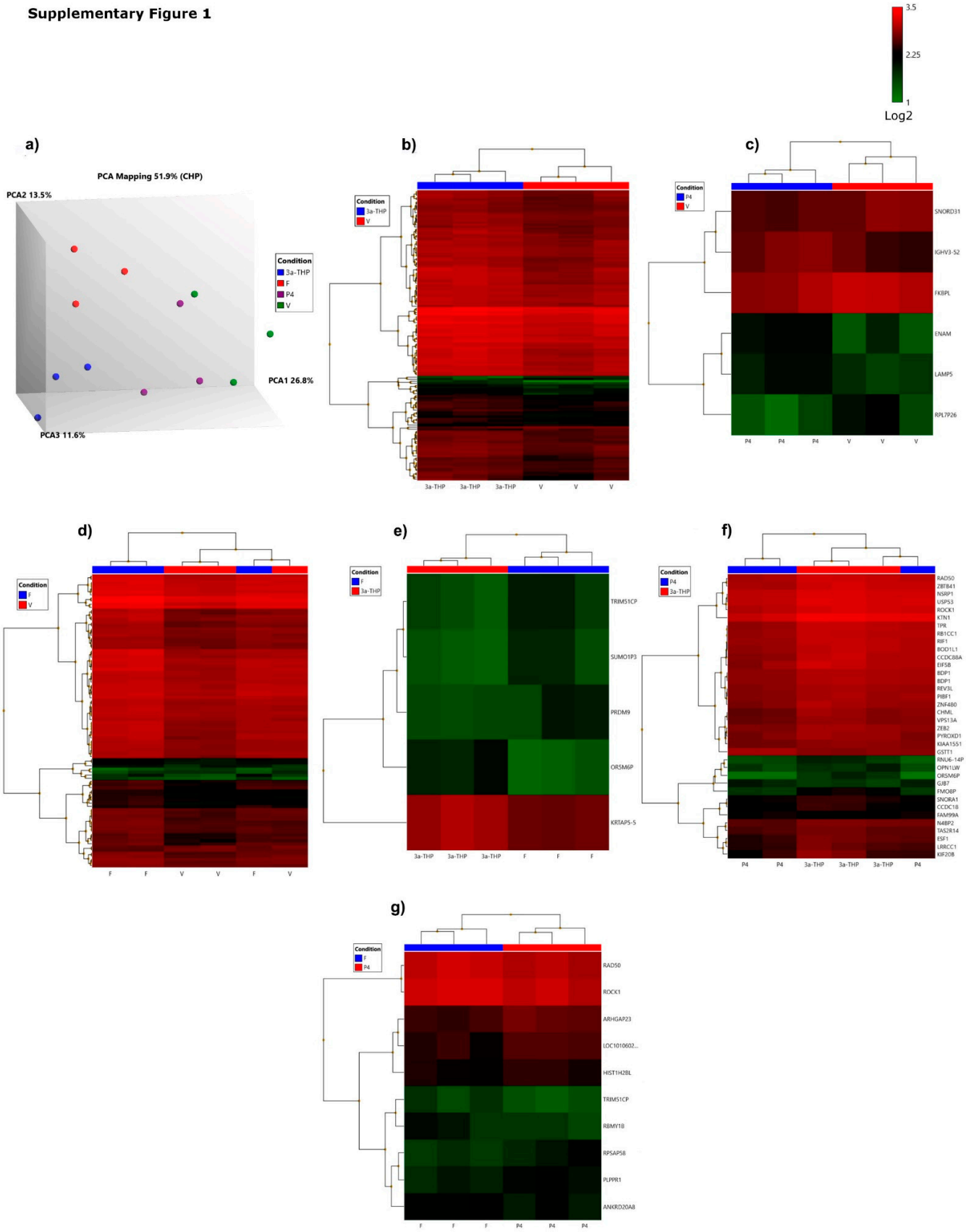

Figure S1. Principal component analysis of microarray data and heat maps of the different comparisons between treatments. **a**) The Principal component analysis shows a tight grouping between treatments: allopregnanolone (3α-THP, blue dots), finasteride (F, red dots), progesterone (P4, purple dots), Vehicle (V, DMSO 0.1 %, green dots). Each axis represents the principal components of the microarray data (PCA1, PCA2, and PCA3), and the variance along each component is indicated; (b–g) Heat maps display the clusters of differentially expressed genes (Fc <-1.5 or >1.5; o p <0.05) between treatments comparisons: **b**) 3α-THP vs V; **c**) P4 vs V; **d**) F vs V; **e**)3α-THP vs F; **f**) 3α-THP vs P4; **g**) P4 vs F. The magnitude of expression of each gene was log2 transformed and represented as indicated in the color scale. Each row represents a gene, and each column represents each sample.

In this section, we show the tables of the differential expressed genes when compared 3α-THP, P4, and F with respect to V, or as a result of the comparisons between treatments. We show results only of annotated genes.

Table S1. Differential gene expression profile of U87 cells treated with 3α-THP vs V.

3α-THP vs V								
Gene Symbol	**Fc**	**P-val**	**Gene Symbol**	**Fc**	**P-val**	**Gene Symbol**	**Fc**	**P-val**
OR5M6P	2.26	5.28E-06	ROCK2	1.94	0.0102	PHF3	2.19	0.0218
RALGAPA1	1.52	0.0004	THOC2	1.52	0.0104	ATRX	2.34	0.0222
DLEU2	1.61	0.0004	BST2	-1.63	0.0105	ZNF292	1.82	0.0223
ARID4B	1.62	0.0006	BDP1	1.72	0.0105	NOL8	1.51	0.0227
ZNF107	1.6	0.0008	BDP1	1.71	0.011	MAP9	2.09	0.0235
CLEC2D	1.54	0.0019	OR4F14P	1.54	0.011	CCDC82	2.09	0.0237
LOC105374874	1.97	0.002	EIF5B	2.85	0.0111	CEP135	1.71	0.0246
SCAF11	1.53	0.0024	CHML	2.37	0.0115	ERV3-1; ZNF117	1.77	0.0248
RAD50	2.31	0.0031	OCR1	1.69	0.0116	CEP295	1.71	0.0249
KIAA2026	1.6	0.0031	ESCO1	1.63	0.0116	ETAA1	1.66	0.0249
TAS2R50	1.71	0.0032	NBEAL1	1.51	0.0116	CNTLN	1.64	0.0253
ESF1	3.07	0.0032	USP53	1.82	0.0119	SMC4	2.24	0.0254
SNORA1; TAF1D; SNORA8	1.89	0.0032	SMC5	1.53	0.012	GOLGA4	1.93	0.0254
ZEB2	1.63	0.0038	EXOC5	1.55	0.0125	SMC3	1.67	0.0261
ROCK1	1.94	0.004	ZNF480	2.15	0.0126	RBMY1B; RBMY1D; RBMY1E	1.74	0.0267
RBM41	1.82	0.0044	GCC2	1.94	0.0131	DST	2	0.0274
DYNC2H1	1.64	0.0046	OR4F29; OR4F3; OR4F16; OR4F21	1.52	0.0132	RBBP6	1.59	0.0277
REV3L	1.86	0.0049	BAZ2B	1.54	0.0132	CEP152	1.98	0.0278
ZNF267	1.97	0.0049	SLK	1.77	0.0133	TRNT1	1.51	0.028
CEP112	1.5	0.005	CWC22	1.51	0.014	TRIP11; ATXN3	2.16	0.0285
PPIG	2.05	0.0051	SAMD9	2.7	0.014	APC	1.87	0.0299
NEMF	1.92	0.0051	VPS13A	2.15	0.0145	GOLGB1	1.77	0.0309
RB1CC1	2.46	0.0054	JMJD1C	1.85	0.0145	PCGF5	1.58	0.0312
PIBF1	1.69	0.0054	MMP16	1.61	0.0147	ARID4A	1.7	0.0312

RIF1	2.69	0.0055	RGPD1; RGPD6; RGPD5; RGPD4; RGPD8; RGPD2	1.5	0.0148	ZNF644	1.62	0.0324
MANEA	1.52	0.0057	TAS2R19; TAS2R30	1.99	0.0151	OR4F15	1.6	0.0328
KIAA1551	1.57	0.006	CCDC18	1.7	0.0151	PHIP	1.7	0.0329
NSRP1	1.62	0.0063	VPS13C	1.7	0.0154	KIF20B	3.25	0.0346
TPR	2.75	0.0063	RBM7	-1.58	0.0158	RPL7P26	-1.77	0.0366
CCDC88A	2.97	0.0064	UACA	1.68	0.0159	HNRNPU	1.69	0.0372
ZNF638	1.56	0.0067	NIPBL	2.25	0.0167	FMO8P	1.56	0.038
CCDC186; MIR2110	2.48	0.0067	RNU6-79P	1.68	0.0169	DCUN1D1	1.53	0.0383
ODF2L	1.54	0.0068	ATRX	1.91	0.0172	HEXA-AS1	1.51	0.0391
LRRCC1	2.17	0.007	MIS18BP1	2.95	0.0173	RANBP2	1.87	0.0405
ZC3H13	1.94	0.0072	ANKRD30B	1.53	0.0177	ANKRD36B	1.56	0.0405
TAS2R31	2.32	0.0074	ENAM	1.67	0.0183	SMC2	2.27	0.0406
FAM216B	1.62	0.0078	EEA1	2.42	0.0187	MIR186	1.87	0.0421
MNS1	2.46	0.008	ACAA1	-1.64	0.0188	ANKRD36; ANKRD36B	1.57	0.0423
FAM99A	-1.61	0.0081	IFT74	1.71	0.0192	CHD1	1.9	0.0433
PCM1	1.68	0.0082	PIK3C2A	1.71	0.0194	NPAT	1.56	0.0435
KTN1	2.68	0.0086	CASP8AP2	2.18	0.0195	PRO2012	2.02	0.0441
TAS2R14	1.85	0.0086	ANKRD36	1.61	0.0198	SMC6	1.79	0.0449
BOD1L1	2.22	0.0095	KIF18A	2.52	0.0201	ZNF518A	1.63	0.0451
ZBTB41	1.95	0.0095	ANKRD36; ANKRD36C	1.53	0.0209	TAS2R13	1.53	0.0454
N4BP2	1.9	0.0097	LPAR4	1.54	0.0212	SLC16A7	1.53	0.0486
HMGN5	1.64	0.0099	CEBPZ	1.54	0.0216	FAR1	1.51	0.0489
						KCNT2	1.63	0.0499

Note: Fc = Fold change

Table S2. Differential gene expression profile of U87 cells treated with P4 vs V.

P4 vs V								
Gene Symbol	**Fc**	**P-val**	**Gene Symbol**	**Fc**	**P-val**	**Gene Symbol**	**Fc**	**P-val**
ENAM	2.27	0.0015	FKBPL	-1.5	0.0131	SNORD31; SNHG1	-1.51	0.0189
LAMP5	1.53	0.0041	FKBPL	-1.5	0.0131	IGHV3-52; IGHV3-33; IGHV3-35; IGHV3-38	1.65	0.0289
						RPL7P26	-1.9	0.0448

Table S3. Differential gene expression profile of U87 cells treated with F vs V.

F vs V								
Gene Symbol	**Fc**	**P-val**	**Gene Symbol**	**Fc**	**P-val**	**Gene Symbol**	**Fc**	**P-val**
BIVM	-1.53	0.0027	NEMF	1.73	0.0168	PIK3C2A	1.63	0.029
CEP112	1.72	0.0029	GCC2	2.74	0.0171	ZBTB20	1.66	0.0291
SCAF11	1.53	0.0044	KTN1	2.55	0.0177	ANKRD36; ANKRD36C	1.72	0.0299
CEP162	1.62	0.005	LRRCC1	1.95	0.0186	OR7E121P	-1.63	0.0307
ANKRD36	1.81	0.0055	SLK	1.8	0.0196	VPS13C	1.64	0.0312
RNU5A-1	-1.52	0.0057	TPR	2.59	0.02	LOC100287934	1.6	0.0327
RAD50	2.16	0.0061	PCM1	1.54	0.0204	ZNF292	2.13	0.0333
ZNF37A	1.58	0.0065	ZEB2	1.53	0.0204	MAP9	2.15	0.0338
ZNF721; ABCA11P	1.67	0.0066	CCDC88A	2.86	0.0205	TMF1	1.59	0.0339
RBMY1B; RBMY1D; RBMY1E	2.01	0.0066	NBEAL1	1.55	0.0205	ENAM	1.66	0.0349
MANEA	1.52	0.0071	ANKRD30 B	1.7	0.021	CEP135	1.58	0.0353
TRIM51CP	1.72	0.0074	TEX9	1.67	0.0214	CASP8AP2	2.14	0.0361
RBM41	1.9	0.0075	ADAM28	1.51	0.0215	ATRX	2.37	0.0364
ROCK1	2.04	0.008	CHD9	1.57	0.0221	EIF5B	2.23	0.0367
SNORA1; TAF1D; SNORA8	1.57	0.0085	RIF1	2.34	0.0223	RBBP6	1.56	0.0384
KIAA2026	1.56	0.0087	ESCO1	1.78	0.0225	OCR1	1.54	0.0394
DYNC2H1	1.55	0.0091	ZNF267	1.67	0.0227	LOC100287934; LOC100287497	1.61	0.0396
CCDC186; MIR2110	2.83	0.0097	ZC3H13	1.74	0.023	ATRX	2.91	0.0396
ANKRD20A8P; ANKRD20A2	1.53	0.0099	SAMD9	3.07	0.0234	PHF3	2.32	0.0408
LIPK	-1.62	0.01	ESF1	2.01	0.0248	ARID4A	1.8	0.0412
PIBF1	1.59	0.01	UACA	1.96	0.0253	LPAR4	1.54	0.0424
OR4F14P	1.94	0.01	JMJD1C	1.99	0.0259	GOLGA4	1.77	0.0424
RB1CC1	2.46	0.0101	BDP1	1.68	0.026	NBEAL1	1.57	0.0429
PWAR6	1.65	0.0113	BOD1L1	2.05	0.0262	ANKRD20A12P	2.02	0.0433
TAS2R31	2.23	0.0116	BDP1	1.71	0.0263	ANKRD20A12P	1.84	0.0437
TAS2R50	1.72	0.0116	BAZ2B	1.59	0.0266	APC	1.88	0.0445
ZNF638	1.51	0.0122	EEA1	2.39	0.027	SAMD9L	1.86	0.0454
PPIG	1.9	0.0123	MNS1	1.73	0.0275	TRIP11; ATXN3	2.21	0.0457
HMGN5	1.56	0.0132	CCDC14	1.51	0.0288	MIS18BP1	2.46	0.0462
REV3L	1.83	0.0139	N4BP2	1.83	0.0288	PHIP	1.82	0.0463
ROCK2	1.8	0.0152	ZBTB41	1.89	0.029	VPS13A	1.75	0.0464
						NIPBL	2.16	0.0483

Table S4. Differential gene expression profile of U87 cells treated with 3α-THP vs P4.

3α-THP vs P4								
Gene Symbol	**Fc**	**P-val**	**Gene Symbol**	**Fc**	**P-val**	**Gene Symbol**	**Fc**	**P-val**
OR5M6P	2.05	1.22E-05	PYROXD1	1.58	0.0207	KIF20B	2.26	0.0377
FMO8P	2.38	0.0033	KIAA1551	1.55	0.021	PIBF1	1.6	0.0378
GJB7	-1.5	0.0124	USP53	1.86	0.0221	CHML	1.75	0.0385

NSRP1	1.66	0.0138	TPR	1.95	0.0294	N4BP2	1.71	0.0391
ESF1	2.13	0.0141	BDP1	1.69	0.0298	KTN1	1.85	0.0393
SNORA1; TAF1D; SNORA8	1.68	0.0154	BOD1L1	1.73	0.0301	ZNF480	1.61	0.0401
ZEB2	1.7	0.0161	REV3L	1.51	0.0322	OPN1LW	1.51	0.0417
CCDC18	1.82	0.0161	RIF1	2.05	0.0326	RB1CC1	1.68	0.0425
RNU6-14P	1.7	0.0166	BDP1	1.68	0.0327	FAM99A	-1.61	0.0427
RAD50	1.7	0.0166	ZBTB41	1.82	0.0334	GSTT1	-1.51	0.0452
ROCK1	1.54	0.0169	CCDC88A	2.33	0.0355	TAS2R14	1.52	0.0458
LRRCC1	1.86	0.0203	EIF5B	1.88	0.0367	VPS13A	1.72	0.0489

Table S5. Differential gene expression profile of U87 cells treated with 3α-THP vs F.

3α-THP vs F					
Gene Symbol	**Fc**	**P-val**	**Gene Symbol**	**Fc**	**P-val**
OR5M6P	1.83	4.49E-05	TRIM51CP	-1.68	0.0086
KRTAP5-5	1.63	0.0006	PRDM9	-1.63	0.0392
			SUMO1P3	-1.65	0.0396

Table S6. Differential gene expression profile of U87 cells treated with P4 vs F.

P4 vs F								
Gene Symbol	**Fc**	**P-val**	**Gene Symbol**	**Fc**	**P-val**	**Gene Symbol**	**Fc**	**P-val**
ARHGAP23	1.6	0.0047	RBMY1B; RBMY1D; RBMY1E	-1.59	0.0255	RPSAP58	1.76	0.0381
TRIM51CP	-1.58	0.0148	RAD50	-1.59	0.035	HIST1H2BL	1.51	0.0385
LOC101060256	1.6	0.0166	ROCK1	-1.63	0.0354	ANKRD20A8P; ANKRD20A12P	-1.54	0.0419
						PLPPR1	1.6	0.0495

Table S7. Genes chosen for validation.

Gene full name and locus	Gene product characteristics and function
ESF1: ESF1 nucleolar pre-rRNA processing protein homolog 20p12.1	ESF1 (also called ABTAP) codes for an evolutionarily conserved nucleolar protein that is part of a system that controls RNA polymerase II-directed transcription. It is involved in the suppression of gene expression by forming a complex with the transcription factor ABT1 [1]. Depletion of the ortholog of this gene in *S. cerevisiae* (Ydr365cp) results in a significant loss of the 18S rRNA, arguing that this protein has discrete domains that mediate direct catalytic functions in the pre-rRNA processing [2]. Furthermore, the functions of nucleolar proteins are tightly linked to cell growth and proliferation [3].
TPR: Translocated promoter region, nuclear basket protein 1q31.1	A protein that forms intracellular filaments anchored to the inner surface of the nuclear pore complex, it forms dimers through its N-terminal domain. TPR is required for the export of mRNA and proteins from the nucleus to the cytoplasm [4]. In the HeLa cell line, TPR silencing promotes cell cycle arrest in G_0/G_1 phase, the appearance of a senescent phenotype, and the accumulation of P53 in the nucleus [5].
RIF1: Replication timing regulatory factor 1	This gene encoding the RIF1 protein was first characterized in yeasts and later was found to be highly conserved among species [6]. RIF1 positively regulates DNA replication [7] and participates in double-strand DNA repair. During anaphase, RIF1 is recruited mainly to the centromeric region, where DNA

2q23.3	strand remains concatenated before topoisomerase II separates the chains. The silencing of RIF1 is associated with micronuclei formation [8]. Also, it is located in aberrant telomeres to promote the repair of the damage [9].
RAD50: RAD50 double-strand break repair protein 5q31.1	The protein encoded by this gene is one of the three components of the MRN complex (Mre11/Rad50/NBS1). The ATPase-nuclease Mer11 and Rad50 are evolutionarily conserved in all organisms [10]. The MRN complex plays a central role in the repair of DNA double-stranded breaks (DSBs), either by homologous recombination (HR) or non-homologous end joining (NHEJ) binding. It also participates in activating the cell cycle ATM checkpoints, the maintenance of telomeres, and meiotic recombination [11]. Mutations in members of the MRN complex are associated with severe phenotypes of cancer susceptibility. In RAD50s/s mice, germline and hematopoietic cell deficiencies are the results of stem cell decay, promoting defects in animal growth, the presence of lymphomas and predisposition to cancer [12,13]. Besides, it has also been found that the expression of RAD50 is increased in melanoma [14].
ROCK1: Rho-associated coiled-coil containing protein kinase 1 18q11.1	This gene encodes for a serine/threonine kinase that keeps 65% of identity with ROCK2 kinase and 92% with the kinase domain of this protein [15]. ROCK1 is an effector of the Rho GTPase and is involved in the phosphorylation of many substrates such as the cytoskeleton protein myosin [16]. Overexpression of this gene is correlated with an increase in cell proliferation, invasion, migration, and metastasis of human lung and breast cancer cell lines as well as GBMs [17–19].
ROCK2: Rho-associated coiled-coil containing protein kinase 22p25.1	The protein encoded by this gene is a serine/threonine kinase of the same family as ROCK1. It regulates cytokinesis, the formation of actin fibers, and the activation of c-fos response factor. It is associated with actin microfilaments as well as with the stress fibers of growing cells [19,20]. Contrary to ROCK1, ROCK2 is mainly expressed in the CNS [21].
REV3L: REV3-like, DNA directed polymerase zeta catalytic subunit 6q21	REV3L is the orthologous gene of the *S. cerevisiae* REV3 gene encoding the catalytic subunit of the DNA polymerase ζ. It is highly conserved in mammals and is indispensable during development, its deletion in mice causes embryonic death [22]. DNA polymerase ζ is a heterotetramer constituted by a REV3 heterodimer, REV7 and two accessory proteins that are shared with the Pol δ [23]. Implicated in double-strand DNA break repair, lacks 3′-5′exonuclease activity and maintains the genome integrity at the expense of the introduction of mutations in the genome. Hence, it is associated with the tumorigenic potential of the cells and/or the progression of cancer [24]. Besides, the conditional knockout mice for REV3L show spontaneous tumors [25].
PCM1: Pericentriolar material 1 protein 8p22	The protein encoded by this gene is a major component of the pericentriolar satellites that determine the centrosomes. It remains attached to the centrosome during G_1, S, and at the beginning of the G_2 phase [26]. PCM1 is essential for the localization of centrosomal proteins and the anchorage of the centrosome microtubules since it recruits the Pkl1 kinase to the pericentriolar material during primary cilia disassembly [27]. Chromosomal aberrations of this gene have been associated with leukemia and pre-menopausal breast cancer [28].
DYNC2H1: Dynein cytoplasmic 2 heavy chain 1 11q22.3	This gene encodes for the heavy chain 1 of the dynein 2 and is found highly conserved among vertebrates, and is widely expressed in ciliated cells. The protein forms homodimers and associates with the light chain intermediated DYNC2LI1 [29]. Has ATPase activity and is involved in the cilia and flagella retrograde transport [30]. Also, it may participate in the protein transport in the Golgi complex, but this has not been fully elucidated [31].
CCDC91: Coiled-coil domain	This protein participates in the protein transport in the Golgi complex. It interacts with monomeric GGA proteins (Golgi-localized, γ-Ear-containing,

containing 91, P56 protein 12q11.22	ADP-ribosylation factor-binding proteins) [32] regulating the trans-Golgi network and endosomal transport [33,34]. It is widely expressed in neuroblastoma, neuroepithelial, melanoma, and fibroblast cell lines.

References

1. Oda, T.; Fukuda, A.; Hagiwara, H.; Masuho, Y.; Muramatsu, M. A.; Hisatake, K.; Yamashita, T. ABT1-associated protein (ABTAP), a novel nuclear protein conserved from yeast to mammals, represses transcriptional activation by ABT1. *J. Cell. Biochem.* **2004**, *93*, 788–806, doi:10.1002/jcb.20114.

2. Peng, W. T.; Krogan, N. J.; Richards, D. P.; Greenblatt, J. F.; Hughes, T. R. ESF1 is required for 18S rRNA synthesis in Sccharomyces cerevisiae. *Nucleic Acids Res.* **2004**, *32*, 1993–1999, doi:10.1093/nar/gkh518.

3. Andersen, J. S.; Lam, Y. W.; Leung, A. K. L.; Ong, S.-E.; Lyon, C. E.; Lamond, A. I.; Mann, M. Nucleolar proteome dynamics. *Nature* **2005**, *433*, 77–83, doi:10.1038/nature03207.

4. Ben-Efraim, I.; Frosst, P. D.; Gerace, L. Karyopherin binding interactions and nuclear import mechanism of nuclear pore complex protein Tpr. *BMC Cell Biol.* **2009**, *10*, 74, doi:10.1186/1471-2121-10-74.

5. David-Watine, B. Silencing Nuclear Pore Protein Tpr Elicits a Senescent-Like Phenotype in Cancer Cells. *PLoS One* **2011**, *6*, e22423, doi:10.1371/journal.pone.0022423.

6. Smogorzewska, A.; de Lange, T. Regulation of telomerase by telomeric proteins. *Annu. Rev. Biochem.* **2004**, *73*, 177–208, doi:10.1146/annurev.biochem.73.071403.160049.

7. Hiraga, S.; Ly, T.; Garzón, J.; Hořejší, Z.; Ohkubo, Y.; Endo, A.; Obuse, C.; Boulton, S. J.; Lamond, A. I.; Donaldson, A. D. Human RIF1 and Protein Phosphatase 1 stimulate DNA replication origin licensing but suppress origin activation. *EMBO Rep.* **2016**, *18*, 403–419, doi:10.15252/embr.201641983.

8. Hengeveld, R. C. C.; de Boer, H. R.; Schoonen, P. M.; de Vries, E. G. E.; Lens, S. M. A.; van Vugt, M. A. T. M. Rif1 Is Required for Resolution of Ultrafine DNA Bridges in Anaphase to Ensure Genomic Stability. *Dev. Cell* **2015**, *34*, 466–474, doi:10.1016/j.devcel.2015.06.014.

9. Xu, L.; Blackburn, E. H. Human Rif1 protein binds aberrant telomeres and aligns along anaphase midzone microtubules. *J. Cell Biol.* **2004**, *167*, 819–830, doi:10.1083/jcb.200408181.

10. Hopfner, K. P. ATP puts the brake on DNA double-strand break repair: A new study shows that ATP switches the Mre11-Rad50-Nbs1 repair factor between signaling and processing of DNA ends Prospects & Overviews K.-P. Hopfner. *BioEssays* **2014**, *36*, 1170–1178, doi:10.1002/bies.201400102.

11. van den Bosch, M.; Bree, R. T.; Lowndes, N. F. The MRN complex: coordinating and mediating the response to broken chromosomes. *EMBO Rep.* **2003**, *4*, 844–9, doi:10.1038/sj.embor.embor925.

12. Bender, C. F.; Sikes, M. L.; Sullivan, R.; Huye, L. E.; Beau, M. M. Le; Roth, D. B.; Mirzoeva, O. K.; Oltz, E. M.; Petrini, J. H. J. Cancer predisposition and hematopoietic failure in Rad50 S / S mice. *Genes Dev.* **2002**, *16*, 2237–2251, doi:10.1101/gad.1007902.like.

13. de Jager, M.; Kanaar, R. Genome instability and Rad50(S): subtle yet severe. *Genes Dev.* **2002**, *16*, 2173–2178, doi:10.1101/gad.1025402.

14. Avaritt, N. L.; Owings, R.; Reynolds, M.; Larson, S. K.; Byrum, S.; Hiatt, K. M.; Smoller, B. R.; Tackett, A. J.; Cheung, W. L. Misregulation of Rad50 expression in melanoma cells. *J. Cutan. Pathol.* **2012**, *39*, 680–684, doi:10.1111/j.1600-0560.2012.01915.x.

15. Chin, V. T.; Nagrial, A. M.; Chou, A.; Biankin, A. V; Gill, A. J.; Timpson, P.; Pajic, M. Rho-associated kinase signalling

and the cancer microenvironment: novel biological implications and therapeutic opportunities. *Expert Rev. Mol. Med.* **2015**, *17*, e17, doi:10.1017/erm.2015.17.

16. Julian, L.; Olson, M. F. Rho-associated coiled-coil containing kinases (ROCK): structure, regulation, and functions. *Small GTPases* **2014**, *5*, e29846, doi:10.4161/sgtp.29846.

17. Zohrabian, V. M.; Forzani, B.; Chau, Z.; Murali, R.; Jhanwar-Uniyal, M. Rho/ROCK and MAPK signaling pathways are involved in glioblastoma cell migration and proliferation. *Anticancer Res.* **2009**, *29*, 119–23.

18. Li, B.; Zhao, W.-D.; Tan, Z.-M.; Fang, W.-G.; Zhu, L.; Chen, Y.-H. Involvement of Rho/ROCK signalling in small cell lung cancer migration through human brain microvascular endothelial cells. *FEBS Lett.* **2006**, *580*, 4252–4260, doi:10.1016/j.febslet.2006.06.056.

19. Hsu, C.-Y.; Chang, Z.-F.; Lee, H.-H. Immunohistochemical evaluation of ROCK activation in invasive breast cancer. *BMC Cancer* **2015**, *15*, 943, doi:10.1186/s12885-015-1948-8.

20. Katoh, K.; Kano, Y.; Noda, Y. Rho-associated kinase-dependent contraction of stress fibres and the organization of focal adhesions. *J. R. Soc. Interface* **2011**, *8*, 305–311, doi:10.1098/rsif.2010.0419.

21. Yin, H.; Hou, X.; Tao, T.; Lv, X.; Zhang, L.; Duan, W. Neurite outgrowth resistance to rho kinase inhibitors in PC12 Adh cell. *Cell Biol. Int.* **2015**, *39*, 563–576, doi:10.1002/cbin.10423.

22. Makarova, A. V.; Burgers, P. M. Eukaryotic DNA polymerase ζ. *DNA Repair (Amst).* **2015**, *29*, 47–55, doi:10.1016/j.dnarep.2015.02.012.

23. Baranovskiy, A. G.; Lada, A. G.; Siebler, H. M.; Zhang, Y.; Pavlov, Y. I.; Tahirov, T. H. DNA polymerase δ and ζ switch by sharing accessory subunits of DNA polymerase δ. *J. Biol. Chem.* **2012**, *287*, 17281–17287, doi:10.1074/jbc.M112.351122.

24. Zhu, X.; Zou, S.; Zhou, J.; Zhu, H.; Zhang, S.; Shang, Z.; Ding, W.-Q.; Wu, J.; Chen, Y. REV3L, the catalytic subunit of DNA polymerase ζ, is involved in the progression and chemoresistance of esophageal squamous cell carcinoma. *Oncol. Rep.* **2016**, *35*, 1664–1670, doi:10.3892/or.2016.4549.

25. Wittschieben, J. P.; Patil, V.; Glushets, V.; Robinson, L. J.; Kusewitt, D. F.; Wood, R. D. Loss of DNA polymerase zeta enhances spontaneous tumorigenesis. *Cancer Res.* **2010**, *70*, 2770–2778, doi:10.1158/0008-5472.CAN-09-4267.

26. Balczon, R.; Bao, L.; Zimmer, W. E. PCM-1, a 228-kD centrosome autoantigen with a distinct cell cycle distribution. *J. Cell Biol.* **1994**, *124*, 783–793, doi:10.1083/jcb.124.5.783.

27. Wang, G.; Chen, Q.; Zhang, X.; Zhang, B.; Zhuo, X.; Liu, J.; Jiang, Q.; Zhang, C. PCM1 recruits Plk1 to the pericentriolar matrix to promote primary cilia disassembly before mitotic entry. *J. Cell Sci.* **2013**, *126*, 1355–65, doi:10.1242/jcs.114918.

28. Armes, J. E.; Hammet, F.; de Silva, M.; Ciciulla, J.; Ramus, S. J.; Soo, W.-K.; Mahoney, A.; Yarovaya, N.; Henderson, M. a; Gish, K.; Hutchins, A.-M.; Price, G. R.; Venter, D. J. Candidate tumor-suppressor genes on chromosome arm 8p in early-onset and high-grade breast cancers. *Oncogene* **2004**, *23*, 5697–702, doi:10.1038/sj.onc.1207740.

29. Mikami, A.; Tynan, S. H.; Hama, T.; Luby-Phelps, K.; Saito, T.; Crandall, J. E.; Besharse, J. C.; Vallee, R. B. Molecular structure of cytoplasmic dynein 2 and its distribution in neuronal and ciliated cells. *J Cell Sci* **2002**, *115*, 4801–4808, doi:10.1242/jcs.00168.

30. Pfister, K. K.; Shah, P. R.; Hummerich, H.; Russ, A.; Cotton, J.; Annuar, A. A.; King, S. M.; Fisher, E. M. C. Genetic analysis of the cytoplasmic dynein subunit families. *PLoS Genet.* **2006**, *2*, 11–26, doi:10.1371/journal.pgen.0020001.

31. Vaisberg, E. A.; Grissom, P. M.; Mclntosh, J. R. Mammalian cells express three distinct dynein heavy chiains that are

colalized to different cytoplasmic organelles. **1996**, *133*, 831–842.

32. Mardones, G. A.; Burgos, P. V.; Brooks, D. A.; Parkinson-Lawrence, Emma Mattera, R.; Bonifacino, J. S. The Trans-Golgi Network Accessory Protein p56 Promotes Long-Range Movement of GGA/Clathrin-containing Transport Carriers and Lysosomal Enzyme Sorting. *Mol. Biol. Cell* **2007**, *18*, 3486–3501, doi:10.1091/mbc.E07.

33. Bonifacino, J. S. The GGA proteins: adaptors on the move. *Nat Rev Mol Cell Biol* **2004**, *5*, 23–32, doi:10.1038/nrm1279.

34. Ghosh, P.; Kornfeld, S. The GGA proteins: key players in protein sorting at the trans-Golgi network. *Eur. J. Cell Biol.* **2004**, *83*, 257–262, doi:10.1078/0171-9335-00374.